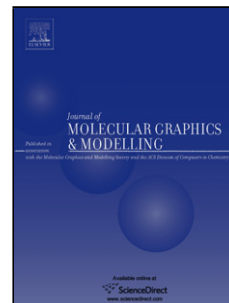


## Accepted Manuscript

Title: Intermolecular hydrogen bonds between 1,4-benzoquinones and HF molecule: synergetic effects, reduction potentials and electron affinities

Authors: Nahid Hesabi, Ali Ebrahimi, Alireza Nowroozi



PII: S1093-3263(17)30446-1  
DOI: <http://dx.doi.org/10.1016/j.jmgm.2017.08.012>  
Reference: JMG 7004

To appear in: *Journal of Molecular Graphics and Modelling*

Received date: 12-6-2017  
Revised date: 10-8-2017  
Accepted date: 11-8-2017

Please cite this article as: Nahid Hesabi, Ali Ebrahimi, Alireza Nowroozi, Intermolecular hydrogen bonds between 1,4-benzoquinones and HF molecule: synergetic effects, reduction potentials and electron affinities, *Journal of Molecular Graphics and Modelling* <http://dx.doi.org/10.1016/j.jmgm.2017.08.012>

This is a PDF file of an unedited manuscript that has been accepted for publication. As a service to our customers we are providing this early version of the manuscript. The manuscript will undergo copyediting, typesetting, and review of the resulting proof before it is published in its final form. Please note that during the production process errors may be discovered which could affect the content, and all legal disclaimers that apply to the journal pertain.

## Intermolecular hydrogen bonds between 1,4-benzoquinones and HF molecule: synergetic effects, reduction potentials and electron affinities

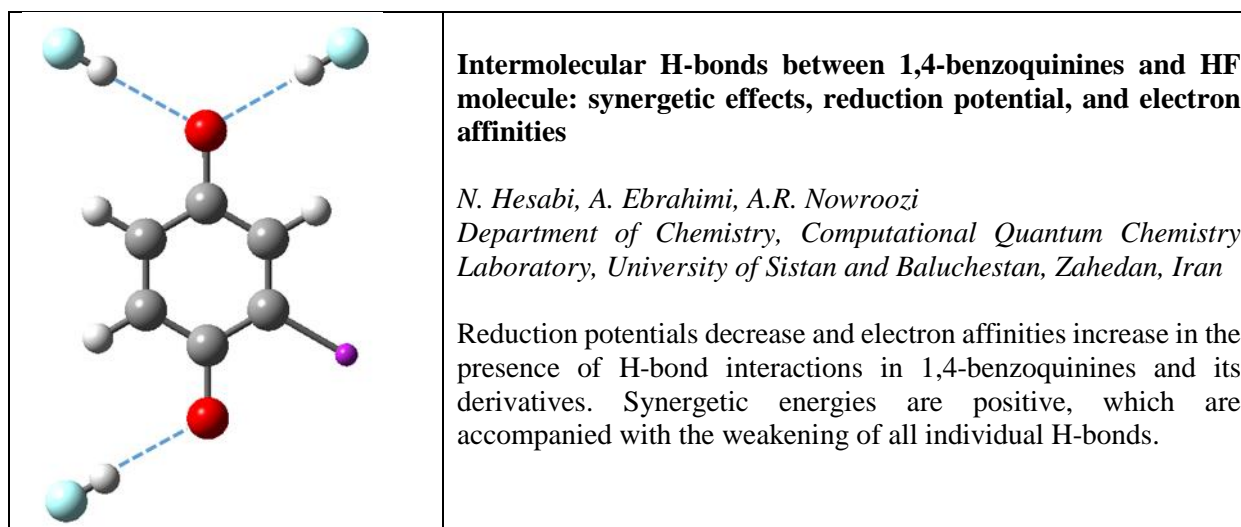
Nahid Hesabi, Ali Ebrahimi\*, Alireza Nowroozi

Department of Chemistry, Computational Quantum Chemistry Laboratory, University of Sistan and Baluchestan, P.O. Box 98135-674, Zahedan, Iran

E-mail: ebrahimi@chem.usb.ac.ir

\* Corresponding author. Fax: +98-541-33446565  
E-mail: ebrahimi@chem.usb.ac.ir (A. Ebrahimi)

### Graphical abstract



### Highlights

- Reduction potentials of 1,4-benzoquinones and its derivatives decrease and their electron affinities increase in the presence of intermolecular H-bonds with positive synergetic energies.

## Abstract

Some biological activities of quinones can be attributed to the H-bonding ability of acceptor oxygen atoms. According to the results obtained from the quantum mechanical calculations performed on a wide variety of complexes between the 1,4-benzoquinone (BQ) derivatives and HF molecules, the interplay between H-bonds and individual H-bond interaction energies ( $E_{\text{HB}}$ ) can be affected by the substituents placed on the six-membered ring of BQ. The total binding energies of complexes become more negative by the electron donating substituents (EDSs) while the changes are reversed by the electron withdrawing substituents (EWSs). The mutual interplay between the  $\text{X-BQ}\cdots(\text{HF})_n$  ( $n= 1-3$ ) interactions has been investigated using the geometrical parameters, synergetic energies (SE) and the  $E_{\text{HB}}$  values. Hydrogen bonding decreases the reduction potentials ( $E_{\text{red}}^0$ ) and increases the electron affinities (EA) of X-BQ derivatives. Linear relationships have been observed between the  $E_{\text{red}}^0$  (and EA) values and the Hammett constants of substituents.

**Keywords:** Intermolecular H-bonding, Synergetic energy, AIM analysis, NPA analysis, 1,4-benzoquinones, Reduction potential, Electron affinity.

## 1. Introduction

The quinone compounds are important in a wide variety of biological processes, such as cellular respiration, photosynthesis, blood coagulation, and tumor growth [1-4]. The quinone family, including anthraquinone, naphthoquinone and benzoquinone, can readily be converted to the hydroquinone anion, via reaction with a hydride anion in a reversible process. They are also capable to accept one or two electrons to form a radical anion ( $\text{Q}^{\cdot-}$ ) or hydroquinone dianion ( $\text{Q}^{2-}$ ). So, they can inhibit the growth of tumors due to the high electron affinities and low redox potentials [5-7]. In

addition to biological activity [8-10], the electron-accepting ability of quinones has a very important role in the organic and inorganic syntheses [11-16]. Benzoquinone derivatives have been specified as electron and proton carriers in photosynthetic and respiratory electron transport chains and as a redox component in the regulation of mitochondrial electron transport [17-22]. These act as primary and secondary electron acceptors in photosynthetic centers [23].

It has been shown that the hydrogen bond formation has an important effect on the structure and activity of quinone compounds in the biological systems [24-27]. The effects of molecular structure and environment on the equilibrium of electron transfer coupled with the H-bonding were obtained from investigation on the reduction potential of quinone systems [28]. The role of each H-bond can be modified by other H-bonds in many chemical and biological systems [29-31].

Recently, the interplay between two or more important non-covalent interactions has been studied in different systems experimentally and theoretically [9,19-33]. Investigation of this effect can be helpful for understanding many biological processes such as binding a drug to the active site of protein. 1,4-benzoquinone (BQ) derivatives are frequently used in many of drug structures. These compounds with four lone pairs of electrons on two oxygen atoms can potentially contribute in four H-bonds as acceptor. The study of synergetic effects can give valuable insights to drug designers when several H-bonds coexist in the BQ complexes.

In this work, the active sites of BQ and its derivatives (X-BQ) were investigated by the quantum mechanical calculations on the quinones and hydrogen bonded complexes illustrated in Scheme 1. The HF molecule is small with one H bond donor, so the O...HF interactions can be studied without additional unsuitable interactions. On the other hand, high electronegativity of F atom makes the mentioned H-bond interaction suitably strong. As can be seen, D1-D3 are binary complexes, T4-T6 are ternary complexes and Q7 is a quaternary complex. Comparison between the results of

calculations obtained for three categories of complexes can be used to investigate the synergetic effects of interactions, the effect of each interaction on the electronic properties of remaining active sites, and the effects of substituents on the active sites of BQ skeleton.

## 2. Computational Methods

The geometry optimization has been performed in the gas phase at the B3LYP/6-311++G(d,p) level using the Gaussian 09 program package [34]. The geometry optimization has also been performed using M06-2X and B3LYP-D3 methods in conjunction with the 6-311++G(d,p) basis set for the binary complexes to examine to what extents will be the differences in geometries optimized using the functionals with and without dispersion correction. The single-point calculations were carried out using the MP2 [35], CCSD [36] and M06-2X [37] methods in conjunction with the 6-311++G(d,p) basis set on the geometries optimized at the B3LYP/6-311++G(d,p) level. The interaction energies were corrected for the basis set superposition error (BSSE) using the counterpoise method of Boys and Bernardi [38]. Topological analysis of electron charge density were carried out using the atoms in molecules method AIM [39] by the AIM2000 [40] program on the wave functions obtained at the B3LYP/6-311++G(d,p) level of theory [41]. Individual H-bond energies ( $E_i$ ) were estimated using the following equation [42]

$$E_i = 100c_i (1 - e^{\rho_i}) \quad \text{eq. 1}$$

where  $\rho_i$  is the electronic charge density calculated at the  $i^{\text{th}}$  H-bond critical point (HBCP) and  $c_i$  is a fitting parameter obtained from a similar equation for a binary complex. The relation between total H-bond energy ( $E_{\text{HB}}$ ) and the individual H-bond energies ( $E_i$ s) is  $E_{\text{HB}}=a_1E_1+a_2E_2$  for ternary complexes and  $E_{\text{HB}}= a_1E_1+a_2E_2+a_3E_3$  for quaternary complexes; herein,  $a_i$ s are also parameters for fitting  $E_{\text{HB}}$  with the  $E_i$  values. In addition, the natural population analysis (NPA) [43] has been performed on the wave functions obtained at the B3LYP/6-311++G(d,p) level by the NBO3.1

program [44] under Gaussian 09 package. The nature of each stationary point was established via the frequency calculations at the B3LYP/6-311++G(d,p) level of theory, the results were used to calculate the Gibbs free energy of compounds and complexes. The redox potentials were also calculated at this level of theory. It is actually preferable to study solution phase phenomena using only solution phase calculations (ie. to calculate free energies in solution based on solution phase geometries, frequencies and energies), rather than involving gas phase results [45]. So, the solvation energies calculated based on solution phase geometries using the solvation model density (SMD) [9,46-48], with the structural relaxation energy also included. The SMD model applies the IEFPCM protocol, and solve the non-homogeneous Poisson equation using a single set of parameters optimized for the IEF-PCM algorithm. In the SMD model, the dispersion and repulsion contributions are calculated using the solvent surface accessible area and atomic surface tensions obtained of electron density [49].

### 3. Results and Discussion

#### 3.1. Geometrical parameters and interaction energies

The most important geometrical parameters, including the O $\cdots$ H bond length and O $\cdots$ H-F bond angle, optimized at B3LYP/6-311++G(d,p) level of theory are given in Table S1, in Supplementary Information (SI). The H-bond lengths are also graphed in Fig. 1 for binary complexes. The O $\cdots$ H bond length is in the range of 1.624-1.782 Å. It increases in the presence of electron withdrawing substituents (EWSs) in the complexes D1 and D2. The changes are reversed in the presence of electron donating substituents (EDSs) in those complexes. Although the changes of mentioned bond length in D3 is similar to those of D1 and D2 in the presence of EWSs, but it increases with EDSs. The H-F $\cdots$ O bond angle lies in the range of 161.34-179.4°; it increases/decreases with EDSs/EWSs. For example, in the presence of most powerful EDS, NHCH<sub>3</sub>, it is equal to 170.58, 171.20 and 170.73

degrees in the complexes D1 - D3, respectively. On the other hand, the most powerful H-bond interaction corresponds to D2 in the presence of NHCH<sub>3</sub> substituent. The lowest H-F...O bond angle (and the weakest O...H bond) is observed in the presence of CN, which is the most powerful EWS, in the complexes D1 - D2. The relationship between the above mentioned geometrical parameters and the electronic properties of substituents can be generalized to the complexes T4-T6 and Q7.

In addition to B3LYP, the geometry optimization were also performed using the B3LYP-D3 and M06-2X methods in conjunction with the 6-311++G(d,p) basis set to examine the differences in geometries optimized using the functionals with and without dispersion correction. The most important geometrical parameters of binary complexes optimized at the mentioned levels are given in Table S2.

The O...H bond length decreases/increases in changing the method from B3LYP to M06-2X/B3LYP-D3 by 0.01-0.03/0.03-0.06 Å. On the other hand, the O...H-F bond angle increases in the changing B3LYP → M06-2X by 3.20-5.99 °. Although the angle decreases in many cases (0.22-1.61 °), but increases in some cases (0.10-1.11 °) in the changing B3LYP → B3LYP-D3.

The total binding energies  $|\Delta E|$  of complexes calculated at the above mentioned level are summarized in Table S3. The BSSE corrected values calculated at the above mentioned level and the MP2, M06-2X and CCSD methods in conjunction with the 6-311++G(d,p) basis set, via the single point calculations are summarized in Tables S4 and S5 in SI. The  $|\Delta E|$  values are also graphed in Fig. 2. As can be seen in Tables S3-S5 and Fig. 2, the  $|\Delta E|$  values obtained at the M06-2X/6-311++G(d,p) and MP2/6-311++G(d,p) levels are higher up to 8 and 16 percent, respectively, than those obtained at the B3LYP/6-311++G(d,p) level, while the values obtained at the CCSD/6-311++G(d,p) level are lower down to 10 percent. Although the  $|\Delta E|$  values depend on the method

selected for calculation, but approximately identical orders are observed for substituents, and also for different positions at various levels of theory.

The trend in the average values of  $|\Delta E|$  calculated at mentioned levels of theory is  $D1 > D2 > D3$ ; the order is poorly maintained constant especially with bulky substituents. Although  $D1 > D3$  is approximately maintained with all substituents,  $D1 > D2$  is not kept in the presence of  $OCH_3$ ,  $NH_2$ , and  $NHCH_3$  substituents and  $D2 > D3$  is not preserved with  $COH$ ,  $COCH_3$ , and  $CONH_2$  substituents. These exceptions are probably related to the steric effects and intramolecular H-bond formation. The H- bonds are strengthened with an EDS (increased interaction energy, decreased H-bond distance) and weakened with an EWS (decreased interaction energy, increased H-bond distance) in the complexes D1 and D2. The steric bulk of the substituent amplifies this effect at the Y2 site. On the other hand, a substituent of either character weakens the H-bond interaction in D3. These results are in agreement with the changes in the molecular electrostatic potential (MEP) around the oxygen atoms (Fig. 3). Blue and red colors indicate positive and negative regions, respectively. It is apparent that the basicity of oxygen atom (O1) involved in D1 and D2 is greater than the O2 one. The EWSs (left) decrease the red negative region, around the oxygen atoms, while the EDSs (right) increase that region around the farther oxygen atom and decrease that around the nearby oxygen. The minimum values of MEP ( $V_{min}$ ) calculated around the O10 are approximately in linear correlation with the  $\Delta E$  values of complexes D1 and D2, while no relationship is observed between the  $\Delta E$  values of D3 and  $V_{min}$  calculated around the O11 atom (see Fig. S2). The electron donation via the resonance effect of substituent is less important in the complexes D3, while the direct interaction of substituent with the oxygen atom decreases the tendency of that atom for interaction with the HF molecule.

The relationship between the  $\Delta E$  values and the electronic properties of substituents has been investigated using the Hammett constants  $\sigma_m$  and  $\sigma_p$ , [50] which can describe the electrostatic and resonance effects, respectively. No linear correlation is observed for  $\Delta E$ - $\sigma_m$  and  $\Delta E$ - $\sigma_p$  pairs. Therefore, the electrostatic and resonance effects are not merely sufficient to predict the trend of the  $\Delta E$  values. The linear relationship of  $\Delta E$  with the sum of Hammett constants of substituents ( $\sigma_{tot} = \sigma_p + \sigma_m$ ) [51,52] has been examined for the complexes D1-D3. Although a good linear correlation is not observed for D3, in which the direct interaction of substituent and the oxygen atom is observed for some substituents, good correlations are observed between the  $\Delta E$  value and  $\sigma_{tot}$  for D1 ( $R^2 = 0.94$ ) and D2 ( $R^2=0.93$ ) that can be seen in Fig. 4. Also, linear correlations are observed between the  $\Delta E$  and  $\sigma_{tot}$  in the complexes T4-T6 and Q7 (see Fig. 5). This indicates that both electrostatic and resonance effects of substituents are vitally important in these intermolecular interactions. In addition, the relationship between the  $|\Delta E|$  values and the electronic properties of substituents has been investigated using the Taft constants  $\sigma^*$  [53,54] for the complexes D1-D3 (Fig. S1). A good linear correlation is not observed when all substituents are considered in the relationship.

### 3.2. Individual hydrogen bond energies

In order to quantify the interplay between two or three H-bonds, the  $\Delta E$  values of ternary and quaternary complexes were weighted using the interaction energies of binary complexes, using individual H-bond energies  $E_{HB}$  estimated for the former cases. The  $E_{HBS}$  of ternary and quaternary complexes were estimated from the  $\rho$  values calculated at the H-BCPs of the complexes. The  $\rho_{H-BCP}$  values obtained from AIM analysis and the estimated  $E_{HBS}$  are given in Tables S6 and S7 in SI. The  $|E_{HB1} + E_{HB3}|$  values in the complexes Q7 are lower than the  $|\Delta E|$  values in the complexes T4 (Table S7). The  $E_{HB}$  values of interactions 1 and 3 estimated in the complexes Q7, T4, D1 and D3 are in consistent with the O $\cdots$ H bond length and also O $\cdots$ H-F bond angle.

The O··H-F bond angle in the complexes D1 and D3 is significantly higher than that in the complexes T4 and Q7. The O··H bond length in the complexes D1 and D3 with one H-bond is shorter than that in the complexes T4 with two H-bonds and Q7 with three H-bonds. In addition, the  $\rho$  values calculated using the AIM analysis at the H-BCPs of the complexes Q7 are lower than those of the complexes T4, D1 and D3 (see Table S6 in SI). The absolute values of  $E_{\text{HB1}}$  and  $E_{\text{HB3}}$  are reduced in average by 9.4% and 2.9%, respectively, in Q7 as compared with those in T4. Thus, the HB2 interaction weakens other two H bonds in the complex Q7, such that the change in HB1 is higher than that in HB3. Participation of the second lone pair of O11 in the HB2 formation reduces propensity of the first lone pair in the HB1 formation. Comparison between Q7 and T5 indicates that the  $|E_{\text{HB2}}+E_{\text{HB3}}|$  value generally decreases in the presence of HB1 (Table S7). The order of  $\rho$  values calculated at each H-BCP (HB1, HB2, or HB3) is  $Q7 < T5 < D2$  and  $D3$ .

The values of  $|E_{\text{HB2}}|$  and  $|E_{\text{HB3}}|$  are lower in Q7 as compared to T5 by 7.7 and 4.3 percent in average. Participation of the first lone pair of O11 in the HB1 formation reduces propensity of the second lone pair in the HB2 formation. The estimated values of  $|E_{\text{HB1}}+E_{\text{HB2}}|$  in the complexes Q7 are lower than those in the complexes T6. The estimated  $E_{\text{HB1}}$  and  $E_{\text{HB2}}$  values in the complexes Q7 and T6 are consistent with the O··H-F bond angles and O··H bond lengths. The comparison of  $|E_{\text{HB1}}|$  and  $|E_{\text{HB2}}|$  values in Q7 with those in T6 shows that they decrease by ~4.5 % in average in the presence of HB3. This can be generalized to other complexes; the absolute value of each  $E_{\text{HB}}$  in T4-T6 is lower than that in D1-D3 by 5-10 percent in average.

### 3.3. Synergetic energies

The mutual interplay of H-bonds can be considered in terms of a practical parameter that is called synergetic energy (SE) [55-58]. Some SE values have been calculated by the following equation (see Table S8)

$$SE_i = \Delta E - \sum \Delta E_{\text{bin}} \quad i=1-4 \quad \text{eq. 2}$$

where  $\Delta E$  is the complexation energy of a ternary or quaternary complex and  $\Delta E_{\text{bin}}$ s are the complexation energies in related binary complexes. The  $SE_5$  to  $SE_7$  values have been calculated by the following equation

$$SE_i = \Delta E_Q - (\Delta E_{T_j} + \Delta E_{D_k}) \quad i=5-7 \quad \text{eq. 3}$$

where  $T_j/D_k$  pair is  $T_4/D_2$ ,  $T_6/D_3$  and  $T_5/D_1$  for  $SE_5$ ,  $SE_6$  and  $SE_7$ , respectively.

As can be seen in Table S8 and Fig. 6, all  $SE_1$ - $SE_7$  values are positive, which confirm negative synergetic effects when two or three H-bonds coexist in the complexes. Positive synergetic energies are in agreement with the geometrical parameters. A positive SE can be accompanied with the weakening of all or some individual H-bonds. What is happened can be specified from the estimated individual H-bonds energies. The SE values are in good agreement with the geometrical parameters of the complexes and the results of AIM analysis.

### 3.4. The natural bond orbital (NBO) analysis

The effects of interactions on the electronic nature of H-bond acceptors have also been investigated via the NBO analysis [43]. The energy values of the most important donor-acceptor interaction  $lp_{\text{O}} \rightarrow \sigma_{\text{HF}}^*$ ,  $E^2$ , and the natural charges calculated on the bridged hydrogen atoms,  $q_{\text{H}}$ , calculated at the B3LYP/6-311++G(d, p) level of theory are given in Tables 1 and S9, respectively.

The CT values estimated on the basis of atomic charges ( $\sum q$ ) of the X-BQ fragments are reported in Table 1. As can be seen, CT is occurred from BQ to the HF molecule; it is higher in the presence of EDSs. The highest/lowest CT corresponds to  $\text{NHCH}_3/\text{CN}$  substituent in the complexes D1-Q7. A linear correlation is observed between CT and the  $\sum \rho_{\text{BCP}}$  values calculated at the  $\text{O} \cdots \text{H}$  BCPs. The CT value is higher in Q7 as compared to the complexes D1-D3 and T4-T6.

The  $E^2$  value of  $lp_O \rightarrow \sigma_{HF}^*$  interaction can be used as a measure of the strength of  $O \cdots H$  interaction. The  $O \cdots H$  bond length decreases/increases in the presence of EDSs/EWSs. The highest/lowest  $E^2$  value corresponds to F/NHCH<sub>3</sub> in the complexes D1 and D2 and COOH/SH in the complex D3. In addition, the highest  $E^2$  value corresponds to NHCH<sub>3</sub> in the complexes T4-T6 and Q7, and the lowest value corresponds to F in the complex T4, COCH<sub>3</sub> in the complexes T5 and Q7, and CN in the complex T6. A linear correlation is observed between CT and  $\sum E^2$  in the ternary and quaternary complexes (see Fig. 7).

The  $q_H$  values and the occupation numbers of  $\sigma_{HF}^*$  orbitals can be used in the investigation of individual HBs. A higher natural charge on the H atom is accompanied by a higher electrostatic contribution in HB. As can be seen in Tables S3-S5, and S9, the  $|\Delta E|$  values increase with increasing the change in the  $q_H$  values. In addition, increase in the  $lp_O \rightarrow \sigma_{HF}^*$  interaction energy enhances the occupation number of  $\sigma_{HF}^*$  and strengthens the H-bond. The highest/lowest occupancy of  $\sigma_{HF}^*$  corresponds to NHCH<sub>3</sub>/CN substituent. The changes of occupation numbers of  $lp_O$  and  $\sigma_{HF}^*$  orbitals are in agreement with the binding energies of complexes.

### 3.5. One-electron reduction potentials

The standard reduction potential ( $E_{red}^0$ ) that measures the propensity of molecules in electron donation and electron acceptance processes, is used in chemical and biological electron-transfer reactions [6]. The  $E_{red}^0$  values are usually measured relative to a reference electrode; the IUPAC had recommended a value of 4.44 eV as the reduction potential of the standard hydrogen electrode SHE in 1986 [9,59].

Although the type of solvent has a significant effect on quinone reactions, they were often considered in water. The electrochemical data of non-aqueous solvents are more limited than those of water solvent [60-63]. The free energy change of the redox process ( $\Delta G_{sol}^*$ ) is used in direct computation

of  $E_{\text{red}}^0$  [10,64-67]. Herein, in order to estimate the one-electron reduction potentials in water, para benzoquinone (P-BQ) is chosen as a reference in the following reaction



where Y is X-BQ or a complex (D1-D3). The reduction potential of Y can be calculated by the following equation

$$E_{\text{red}}^0(Y/Y^{\bullet-}) = E_{\text{red}}^0(\text{P-BQ}/\text{P-BQ}^{\bullet-}) + \Delta G_{\text{sol}}^*/F \quad \text{eq. 5}$$

where  $E_{\text{red}}^0(\text{P-BQ}/\text{P-BQ}^{\bullet-})$  is equal to 4.52 eV in water [68]. The gas phase free energy difference between the ground state and the state with one-electron eliminated from the molecule as well as the solvation free energy of each compound are used to calculate the free energy change of the redox process in the solution

$$\Delta G_{\text{sol}}^* = \Delta G_{\text{g}}^* + \Delta G_{\text{solv}} \quad \text{eq. 6}$$

where

$$\Delta G_{\text{g}}^* = G_{\text{g}}(Y^{\bullet-}) + G_{\text{g}}(\text{p-BQ}) - G_{\text{g}}(Y) - G_{\text{g}}(\text{p-BQ}^{\bullet-}) \quad \text{eq. 7}$$

$G_{\text{g}}(X)$  is the standard Gibbs free energy of compound X in the gas phase, and

$$\Delta G_{\text{solv}} = \Delta G_{\text{solv}}(Y^{\bullet-}) + \Delta G_{\text{solv}}(\text{p-BQ}) - \Delta G_{\text{solv}}(Y) - \Delta G_{\text{solv}}(\text{p-BQ}^{\bullet-}) \quad \text{eq. 8}$$

$\Delta G_{\text{solv}}(X)$  is the solvation energy of compound X.

In addition to the aqueous solution redox potentials, the gas-phase electron affinities (EA) have also been estimated for X-BQ and X-BQ $\cdots$ HF complexes. The EA values were computed using the Gibbs free energy changes of the following process ( $\text{EA} = G_{\text{neutral}} - G_{\text{anion}}$ ) [10].



The EA and  $E_{\text{red}}^0$  values of some X-BQ, as well as D1, D2 and D3 complexes calculated in water at the B3LYP/6-311++G(d,p) level of theory are given in Table S10 and graphed in Fig. 8.

The reduction potential of X-BQ is different from those of the complexes D1-D3. As can be seen in Table S10, the reduction potentials in water are in the range of 2.44 to 5.23, 2.64 to 5.30, 2.70 to 5.20 and 3.45 to 5.84 eV for D1, D2, D3, and X-BQ, respectively. EDSs increase the  $E_{\text{red}}^0$  value significantly, while EWSs decrease that. The EA values are in the range of 47.17 to 79.09, 47.30 to 80.07, 47.24 to 79.84, and 36.55 to 67.95 kcal mol<sup>-1</sup> for D1, D2, D3, and X-BQ, respectively. They decrease in the presence of EDSs, while they increase with EWSs. The  $E_{\text{red}}^0$ /EA value is higher/lower in the X-BQ molecule as compared to the complexes D1-D3.

The ability of X-BQ to capture an electron is lower as compared to the complexes D1-D3; so, lower free energy changes are observed on radical anion formation for X-BQ as compared to the complexes D1-D3 in the gas phase and solution media (see Table 2). They increase/decrease in the presence of EWSs/EDSs. The compounds with more negative  $\Delta G_{\text{sol}}^*$  values are more active on reduction. On the other hand, the H-bond interactions decrease the  $E_{\text{red}}^0$  values in the complexes D1-D3 in comparison with the X-BQ molecules.

The values of  $E_{\text{red}}^0$  and  $\sigma_{\text{tot}}$  are in linear correlations in the complexes D1-D3 ( $E_{\text{red}}^0 = a\sigma_{\text{tot}} + b$ ); herein, a, b, and  $R^2$  are, respectively, equal to -1.09, 3.83, and 0.94 for D1, -1.09, 3.85, and 0.93 for D2, and -1.055, 3.83, and 0.92 for D3 (see Fig. 9). Linear correlations are also observed between the values of EA and  $E_{\text{red}}^0$  ( $E_{\text{red}}^0 = cEA + d$ ); c, d, and  $R^2$  are respectively, equal to -0.08, 8.95 and 0.99 for D1, -0.08, 8.97 and 0.98 for D2, and -0.078, 8.8, and 0.99 for D3.

#### 4. Conclusions

1,4-benzoquinones with four lone pairs of electrons on two oxygen atoms can potentially contribute in four H-bonding as acceptor. In this work, the activities of different positions on the BQ, its derivatives X-BQ, and their complexes with the HF molecule were investigated by quantum mechanical calculation. The results of calculations on the binary (D1-D3), ternary (T4-T6) and

quaternary (Q7) complexes have been used to investigate the synergetic effects of interactions, the effect of each interaction on the electronic properties of remaining active sites, and the effects of substituents on the active sites of BQ skeleton.

The total binding energies of complexes become more negative with EDSs and become less negative in the presence of EWSs. Reliable descriptors have been obtained from good correlations observed for energetic data, geometrical parameters, and some properties obtained from the AIM and NBO analyses with the  $\sigma_{\text{tot}}$  values.

The sum of  $|E_{\text{HB}}|$  values for (1, 3), (2, 3) and (1, 2) pairs of interactions in the quaternary complexes are smaller than the  $|\Delta E|$  values of the complexes T4, T5 and T6, respectively, and the  $|\Delta E|$  values for ternary complexes are smaller than the sum of  $|\Delta E|$  values of related binary complexes. On the other hand, the SE values are positive in the complexes T4-T6 and Q7. Positive SE are accompanied with the weakening of all individual H-bonds. They are in good agreement with the geometrical parameters of the complexes and the results of AIM and NBO analysis.

It is important to bear in mind that any modification of the ring substituents of a benzoquinone will weaken hydrogen bonding to the adjacent oxygen atom; this can be minimised by using an EDS, which has the added advantage of significantly strengthening the hydrogen bonds at the Y1 and Y2 sites. The use of a relatively bulky substituent will confer particular stabilization on the D2 H- bond. The  $E_{\text{red}}^0/\text{EA}$  value of the X-BQ molecule is higher/lower than that of the complexes D1-D3. X-BQ has a lower ability to capture an electron in comparison with the complexes D1-D3 with respect to the free energy changes calculated for the radical anion formation processes.

### **Acknowledgments**

We thank the University of Sistan and Baluchestan for financial supports and Computational Quantum Chemistry Laboratory for computational facilities.

**References**

- [1] B. Prescott, Potential anti-malarial agents derivatives of 2-chloro-1,4-naphthoquinone, *J. Med. Chem.* 12 (1969) 181-182.
- [2] D.E. Wheeler, J.H. Rodriguez, J.K.M. Cusker, Density functional theory analysis of electronic structure variations across the orthoquinone/semiquinone/catechol redox series, *J. Phys. Chem. A* 103 (1999) 4101-4112.
- [3] K. Kapłon, O. Demchuk, M. Wieczorek, K.M Pietrusiewicz, Bronsted acid catalyzed direct oxidative arylation of 1,4-naphthoquinone, *Curr. Chem. Lett.* 3 (2014) 23-36.
- [4] N.G. Clark, The fungicidal activity of substituted 1,4-naphthoquinones, *Pestic. Sci.* 16 (1985) 23-32.
- [5] M. Namazian, P. Norouzi, R. Ranjbar, Prediction of electrode potentials of some quinone derivatives in acetonitrile, *J. Theo. Chem.* 625 (2003) 235-242.
- [6] M. Namazian, L.M. Coote, Accurate calculation of absolute one-electron redox potentials of some para-quinone derivatives in acetonitrile, *J. Phys. Chem. A* 111 (2007) 7227-7232.
- [7] S. Er, C. Suh, M.P. Marshak, A. Aspuru-Guzik, Computational design of molecules for an all-quinone redox flow battery, *Chem. Sci.* 6 (2015) 885-893.
- [8] J.R. Tobias, J. Johnsson, E. Ahlberg, I. Panas, D.J. Schiffrin, Quantum chemical modeling of the reduction of quinones, *J. Phys. Chem. A* 110 (2006) 2005-2020.
- [9] K. Arumugam, U. Becker, Computational redox potential predictions: applications to inorganic and organic aqueous complexes, and complexes adsorbed to mineral surfaces, *Minerals* 4 (2014) 345-387.
- [10] X.Q. Zhu, C.H. Wang, Accurate estimation of the one-electron reduction potentials of various substituted quinones in DMSO and CH<sub>3</sub>CN, *J. Org. Chem.* 75 (2010) 5037-5047.

- [11] R. Salazar, J. Vidal, M.M. Cifuentes, R.A. Maturanac, O.R. Rodriguez, Electrochemical characterization of hydroquinone derivatives with different substituents in acetonitrile, *New J. Chem.* 39 (2015) 1237-1246.
- [12] B.L. Trumpower, *Function of Quinones in Energy Conserving Systems*, Academic Press, New York (1982).
- [13] C. Kirmaier, D. Holten, Photochemistry of reaction centers from the photosynthetic purple bacteria, *Photosynth. Res.* 13 (1987) 225-260.
- [14] J.G. Smith, M. Fieser, *Reagents for Organic Synthesis*, Wiley-Interscience: New-York, 1990.
- [15] S.D.M. Islam, T. Susdorf, A. Penzkofer, P. Hegemann, Fluorescence quenching of flavin adenine dinucleotide in aqueous solution by pH dependent isomerisation and photo-induced electron transfer, *Chem. Phys.* 295 (2003) 137-149.
- [16] J.G. Park, L.R. Jeon, T.D. Harris, Electronic effects of ligand substitution on spin crossover in a series of diimino quinonoid-bridged  $\text{Fe}^{\text{II}}_2$  Complexes, *Inorg. Chem.* 54 (2015) 359-369.
- [17] R.L. Dean, Kinetic studies with alkaline phosphatase in the presence and absence of inhibitors and divalent cations, *Biochem. Mol. Biol. Edu.* 30 (2002) 401-407.
- [18] P. Mitchell, J. Moyle, Translocation of some anions cations and acids in rat liver mitochondria, *Eur J. Biochem.* 9 (1969) 149-155.
- [19] H. Jing, H. Lin, Sirtuins in epigenetic regulation, *Chem. Rev.* 115 (2015) 2350–2375.
- [20] T.E. Allen, B.Q. Palsson, C. Hunte, Sequence-based analysis of metabolic demands for protein synthesis in prokaryotes, *J. Theor. Bio.* 220 (2003) 1-18.
- [21] R. Tao, M.C. Coleman, J.D. Pennington, O. Ozden, S.H. Park, H. Jiang, H.S. Kim, C.R. Flynn, S. Hill, W.H. McDonald, A.K. Olivier, D.R. Spitz, D. Gius, Sirt3-mediated deacetylation of

evolutionarily conserved lysine 122 regulates MnSOD activity in response to stress, *J. Mol. Cell.* 40 (2010) 893-904.

[22] M. Banach, C. Serban, A. Sahebkar, S. Ursoniu, J. Rysz, P. Muntner, P.P. Toth, S.R. Jones, M. Rizzo, S.P. Glasser, G.Y. Lip, S. Dragan, D.P. Mikhailidis, Effects of coenzyme Q10 on statin-induced myopathy, a meta-analysis of randomized controlled trials, *Mayo. Clin. Proc.* 90 (2015) 24-34.

[23] B.A. Diner, V. Petrouleas, J.J. Wendoloski, The iron-quinone electron-acceptor complex of photosystem II, *Physiol. Plant* 81 (1991) 423-436.

[24] R. Ashizawa, T. Noguchi, Effects of hydrogen bonding interactions on the redox potential and molecular vibrations of plastoquinone as studied using density functional theory calculations, *Phys. Chem. Chem. Phys.* 16 (2014) 11864-11876.

[25] P. Beroza, D.R. Fredkin, M.Y. Okamura, G. Feher, Electrostatic calculations of amino acid titration and electron transfer Q-AQB $\rightarrow$ QAQ-B in the reaction center, *Biophys J.* 68 (1995) 2233-2250.

[26] J.P. Klinman, D. Mu, Quinoenzymes in biology, *Annu. Rev. Bio. chem.* 63 (1994) 299-344.

[27] T. Zhang, K. Papson, R. Ochran, D.P. Ridge, Stability of flavin semiquinones in the gas phase: the electron affinity, proton affinity, and hydrogen atom affinity of lumiflavin, *J. Phys. Chem. A* 117 (2013) 11136–11141.

[28] B. Uno, N. Okumura, M. Goto, K. Kano,  $n\text{-}\sigma$  Charge-Transfer interaction and molecular and electronic structural properties in the hydrogen-bonding systems consisting of p-quinone dianions and methyl alcohol, *J. Org. Chem.* 65 (2000) 1448-1455.

[29] W. Wang, Y.Z. hang, K. Huang, Unconventional interaction in N (P) related systems, *Chem. Phy. Lett.* 411 (2005) 439-444.

- [30] A.D. Kulkarni, R.K. Pathak, L.J. Bartolotti, Effect of additional hydrogen peroxide to  $\text{H}_2\text{O}_2 \cdots (\text{H}_2\text{O})_n$   $n = 1$  and 2 complexes: quantum chemical study, *J. Chem. Phys.* 124 (2006), 214309.
- [31] L. Qingzhong, A. Xiulin, L. Feng, L. Wenzuo, G. Baoan, C. Jianbo, S. Jiazhong, Cooperativity between two types of hydrogen bond in  $\text{H}_3\text{C-HCN-HCN}$  and  $\text{H}_3\text{C-HNC-HNC}$  complexes, *J. Chem. Phys.* 128 (2008) 154102.
- [32] F.B. Akher, A. Ebrahimi, Stacking effects on the hydrogen bonding capacity of methyl-2-naphthoate, *J. Mol. Graph. Mod.* 61 (2015) 115–122.
- [33] S. Sarhadinia, A. Ebrahimi, H-bond and dipole–dipole interactions between water and COO functional group in methyl benzoate derivatives: Substituent and heteroatom effects, *J. Mol. Graph. Mod.* 70 (2016) 7–13.
- [34] M.J. Frisch, et al, Gaussian 09, Revision A.02, Gaussian Inc, Wallingford, CT, 2009.
- [35] C. Møller, M.S. Plesset, Note on an approximation treatment for many-electron systems, *Phys. Rev.* 46 (1934) 618-622.
- [36] K. Raghavachari, G.W. Trucks, J.A. Pople, M. Head-Gordon, A fifth-order perturbation comparison of electron correlation theories, *Chem. Phys. Lett.* 157 (1989) 479-483.
- [37] E.G. Hohenstein, S.T. Chill, C.D. Sherrill, Assessment of the performance of the M05-2X and M06-2X exchange correlation functionals for noncovalent interactions in biomolecules, *J. Chem. Theory Comput.* 4 (2008) 1996-2000.
- [38] S.F. Boys, F. Bernardi, The Calculation of small molecular interactions by the differences of separate total energies some procedures with reduced errors, *Mol. Phys.* 19 (1970) 553-566.
- [39] R.F.W. Bader, *Atoms in Molecules: A Quantum Theory*, Oxford University Press, Oxford, 1990.

- [40] K.F. Biegler, J. Schonbohm, D. Bayles, AIM2000-a program to analysis and visualize atoms in molecules, *J. Comput. Chem.* 22 (2001) 545-559.
- [41] P. Politzer, F. Abu-Awwad, A comparative analysis of Hartree-Fock and Kohn-Sham Orbital Energies. *Theor. Chem. Acc.* 99 (1998) 83-87.
- [42] A. Ebrahimi, S.M. Habibi Khorassani, H. Delarami, Estimation of individual binding energies in some dimers involving multiple hydrogen bonds using topological properties of electron charge density, *Chem. Phys.* 365 (2009) 18-23.
- [43] A.E. Reed, R.B. Weinstock, F. Weinhold, Natural population analysis, *J. Chem. Phys.* 83 (1985) 735-746.
- [44] E.D. Glendening, A.E. Reed, J.E. Carpenter, F. Weinhold, NBO Version 3.1. Theoretical Chemistry Institute, University of Wisconsin, Madison, 1990.
- [45] J. Ho, Are thermodynamic cycles necessary for continuum solvent calculation of pK<sub>a</sub>s and reduction potentials? *Phys. Chem. Chem. Phys.* 17 (2015) 2859.
- [46] E. Cancès, B. Mennucci, J. Tomasi, A new integral equation formalism for the polarizable continuum model, theoretical background and applications to isotropic and anisotropic dielectrics, *J. Chem. Phys.* 107 (1997) 3032-3041.
- [47] E.J. Bachman, A.L. Curtiss, S.A. Rajeev, Investigation of the redox chemistry of anthraquinone derivatives, using density functional theory, *J. Phys. Chem. A* 118 (2014) 8852-8860.
- [48] J. Berges, P. Oliveira, I. Fourré, C. Houee-Levin. The one-electron reduction potential of methionine-containing peptides depends on the sequence. *J. Phys. Chem. B* 116 (2012) 9352-9362.
- [49] A.V. Marenich, C.J. Cramer, D.G. Truhlar, Universal solvation model based on solute electron density and on a continuum model of the solvent defined by the bulk dielectric constant and atomic surface tensions, *J. Phys. Chem. B*, 2009, 113, 6378–6396.

- [50] C. Hansch, A. Leo, R.W. Taft, A survey of Hammett substituent constants and resonance and field parameters, *Chem. Rev.* 97 (1991) 165-195.
- [51] M. Lewis, C. Bagwill, L.K.E. Hardebeck, S. Wireduaah, The use of hammett constants to understand the non-covalent binding of aromatics, *Comput. Struct. Biotechnol. J.* 1 (2012) 1-9.
- [52] A. Ebrahimi, M. Habibi, R.S. Neyband, A.R. Gholipour, Cooperativity of p-stacking and hydrogen bonding interactions and substituent effect on X-ben||pyr...H-F complexes, *Phys. Chem. Chem. Phys.* 11 (2009) 11424–11431.
- [53] R.W. Taft, Linear Steric Energy Relationships, *J. Am. Chem. Soc.* 75 (1953) 4538–4539.
- [54] W.-Y. Li, O.R. Guo, E.J. Lien, Examination of the interrelationship between aliphatic group dipole moment and polar substituent constants, *Journal of Pharmaceutical Sciences.* 73 (1984) 553-558.
- [55] D. Escudero, A. Frontera, D. Quinonero, P.M. Deya, Interplay between cation- $\pi$  and hydrogen bonding interactions, *Chem. Phys. Lett.* 456 (2008) 257-261.
- [56] L. Yunxiang, L. Yingtao, L. Haiying, Z. Xiang, L. Honglai, Z. Weiliang, Energetic effects between halogen bonds and anion- $\pi$  or lone pair- $\pi$  interactions: A theoretical study, *J. Phys. Chem. A* 116 (2012) 2591-2597.
- [57] X. Lucas, C. Estarellas, D. Escudero, A. Frontera, D. Quonero, P.M. Dey, Very long-range effects: cooperativity between anion- $\pi$  and hydrogen-bonding interactions, *Chem. Phys. Chem.* 10 (2009) 2256-2264.
- [58] M. Solimannejad, A.R. Gholipour, Revealing substituent effects on the concerted interaction of pnictogen, chalcogen, and halogen bonds in substituted s-triazine ring, *Struct. Chem.* 24 (2013) 1705-1711.

- [59] S. Trasatti, The absolute electrode potential, an explanatory note, *Pure Appl. Chem.* 58 (1986) 955-966.
- [60] G.J. Cheng, L.J. Song, Y.F. Yang, X. Zhang, O. Wiest, Y.D. Wu, Computational studies on the mechanism of the copper-catalyzed  $sp^3$ -C-H cross-dehydrogenative coupling reaction, *Chem. Plus. Chem.* (2013) 1-10.
- [61] Y. Fu, L. Liu, Y.M. Wang, J.N. Li, T.Q. Yu, Q.X. Guo, Quantum-Chemical predictions of redox potentials of organic anions in dimethyl sulfoxide and reevaluation of bond dissociation Enthalpies measured by the electrochemical methods, *J. Phys. Chem. A* 110 (2006) 5874-5886.
- [62] T. Liu, M.M. Liu, Y. Li, Z.Y. Yu, Experimental and theoretical study on the redox reaction of noradrenaline on the gold electrode surface, *J. Elec. Chem. Sci.* 11 (2016) 685-691.
- [63] L. Ding, W. Zheng, Y. Wang. Theoretical study on homolytic  $C(sp^2)$ -O cleavage in ethers and phenols, *New J. Chem.* 39 (2015) 6935-6943.
- [64] M.H. Baik, R.A. Friesner, Computing Redox Potentials in Solution: Density Functional Theory as A Tool for Rational Design of Redox Agents, *J. Phys. Chem. A* 106 (2002) 7407-7412.
- [65] M. Schmidt, A. Busch, E.W. Knapp, One-Electron Reduction Potential for Oxygen- and Sulfur-Centered Organic Radicals in Protic and Aprotic Solvents, *J. Am. Chem. Soc.* 127 (2005) 15730-15737.
- [66] P. Winget, E.J. Weber, C.J. Cramer, D.G. Truhlar, Computation of equilibrium oxidation and reduction, *J. Phys. Chem. Chem. Phys.* 2 (2000) 1231-1239.
- [67] N. Jacobs, S. Lang, R. Panisch, G. Wittstock, U. Groth, H.R. Nasiri, Investigation on the electrochemistry and cytotoxicity of the natural product marcanine A and its synthetic derivatives, *RSC Adv.* 5 (2015) 58561-58565.

[68] K.S. Raymond, A.K. Grafton, R.A. Wheeler, Calculated one-electron reduction potentials and solvation structures for selected p-benzoquinones in water, *J. Phys. Chem. B* 101 (1997) 623-631.

**Scheme 1** The binary (Di), ternary (Ti) and quaternary (Q7) complexes.

**Fig. 1** The O...H bond length (in Å) optimized at the B3LYP/6-311++G(d,p) level in the complexes D1-D3.

**Fig. 2** The  $\Delta E$  values calculated using mentioned methods in conjunction with the 6-311++G(d,p) basis set.

**Fig. 3** Electrostatic potentials mapped on the molecular surfaces of BQ (middle), CN-BQ (left), and NHCH<sub>3</sub>-BQ (right).

**Fig. 4** Correlation between  $\Delta E$  and  $\sigma_{\text{tot}}$  for the complexes D1 (▲) and D2 (■).

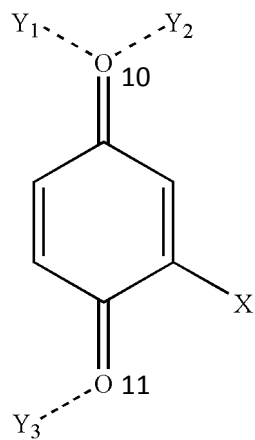
**Fig. 5** Correlation between the binding energies ( $\Delta E$ ) and the Hammett constants ( $\sigma_{\text{tot}}$ ) in the complexes T4 (■), T5 (◆) T6 (●) and Q7 (▲).

**Fig. 6** Synergic energies were calculated using the eqs 2 and 3, where  $SE_1 = \Delta E (T_4) - E (D_1) - E (D_3)$ ,  $SE_2 = \Delta E (T_5) - E (D_2) - E (D_3)$ ,  $SE_3 = \Delta E (T_6) - E (D_1) - E (D_2)$ ,  $SE_4 = \Delta E (Q_7) - E (D_1) - E (D_2) - E (D_3)$ ,  $SE_5 = \Delta E (Q_7) - E (T_4) - E (D_2)$ ,  $SE_6 = \Delta E (Q_7) - E (T_6) - E (D_3)$ ,  $SE_7 = \Delta E (Q_7) - E (T_5) - E (D_1)$ .

**Fig. 7** Correlation between CT and  $\sum E^2$  in the complexes T4-Q7.

**Fig. 8** The reduction potentials ( $E_{\text{red}}^0$ ) and electron affinities (EA) calculated in BQ and the complexes D1-D3.

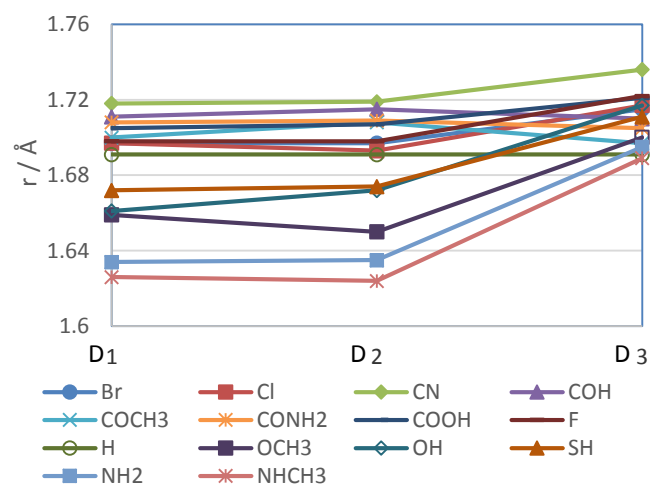
**Fig. 9** Correlation between the reduction potentials ( $E_{\text{red}}^0$ ) and the Hammett constant ( $\sigma_{\text{tot}}$ ) in the complexes D1 (○), D2 (▲) and D3 (■).



- D1: Y1 = HF, Y2 = Y3 = —
- D2: Y2 = HF, Y1 = Y3 = —
- D3: Y3 = HF, Y1 = Y2 = —
- T4: Y1 = Y3 = HF, Y2 = —
- T5: Y2 = Y3 = HF, Y1 = —
- T6: Y1 = Y2 = HF, Y3 = —
- Q7: Y1 = Y2 = Y3 = HF

X=F, Cl, Br, OCH<sub>3</sub>, CN, CONH<sub>2</sub>, COCH<sub>3</sub>, H, NH<sub>2</sub>, NHCH<sub>3</sub>, COOH, OH, SH, COH

### Scheme 1

**Fig. 1**

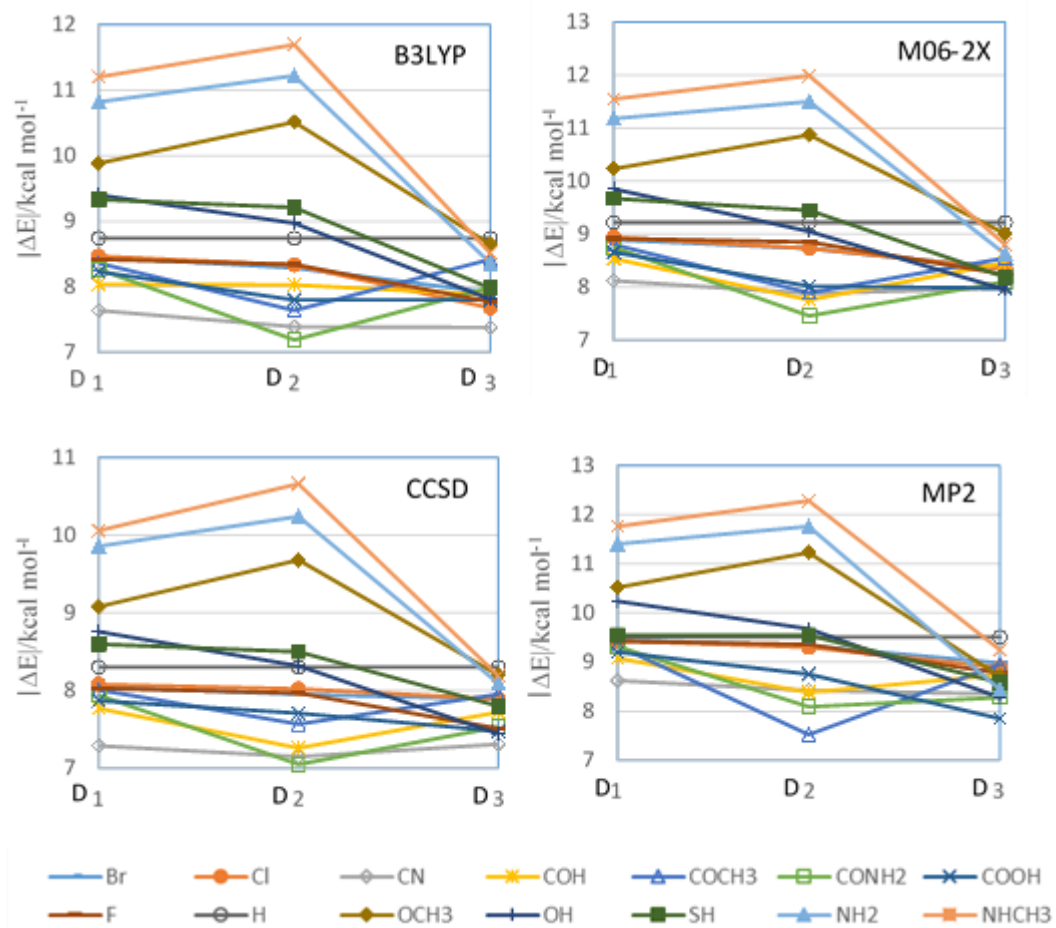
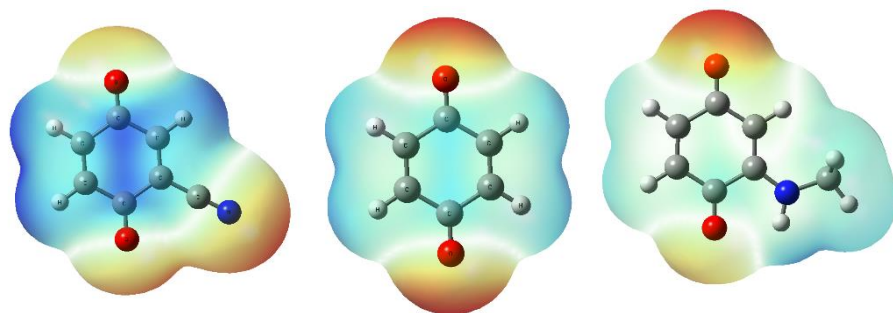
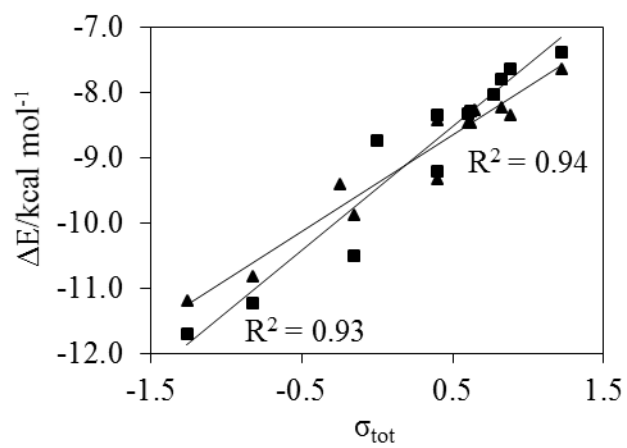
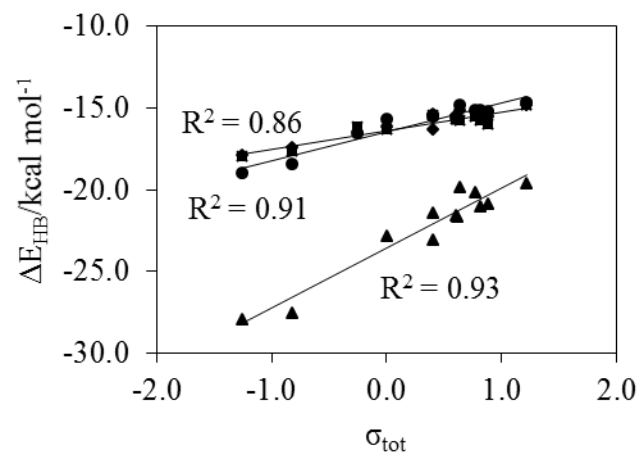


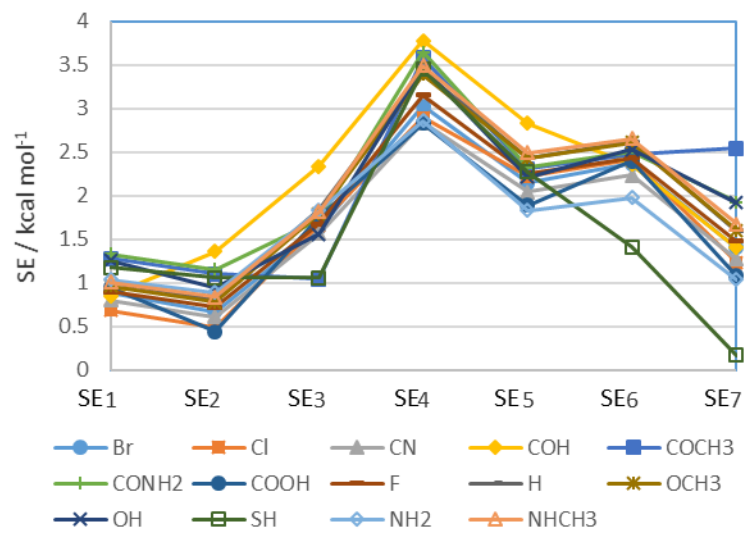
Fig. 2

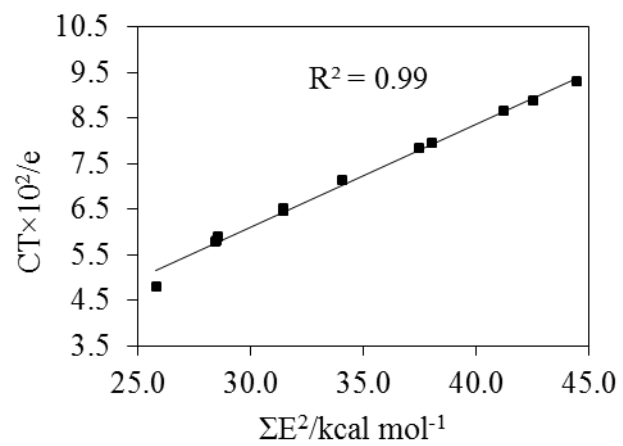


**Fig. 3**

**Fig. 4**

**Fig. 5**

**Fig. 6**

**Fig. 7**

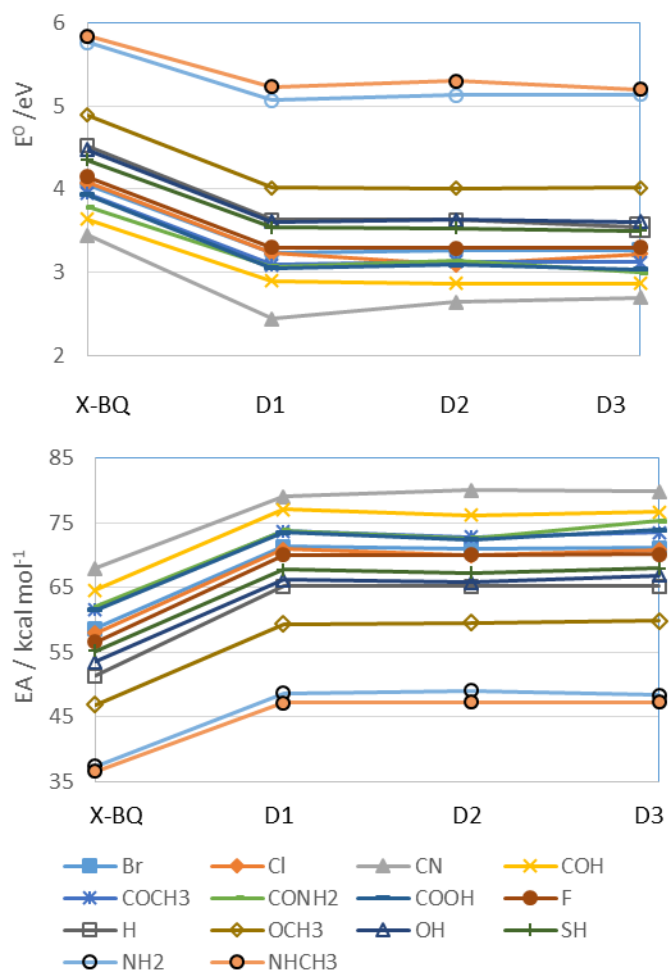
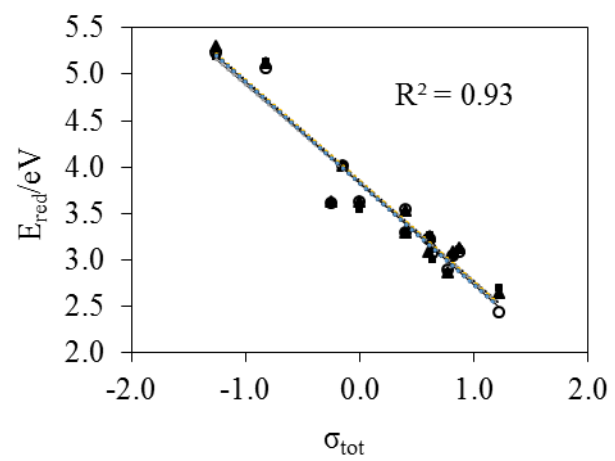


Fig. 8

**Fig. 9**

**Table 1** The results of NBO analysis obtained at the B3LYP6-311++G(d,p) level of theory

X	D1/T4		D2/T5		D3/T6		Q7	
	$\Sigma E^2$	CT $\times 10^2$	$\Sigma E^2$	CT $\times 10^2$	$\Sigma E^2$	CT $\times 10^2$	$\Sigma E^2$	CT $\times 10^2$
Br	27.23, <b>28.25</b>	4.20, <b>5.74</b>	27.35, <b>28.48</b>	4.17, <b>5.80</b>	27.54, <b>30.08</b>	3.80, <b>6.47</b>	36.32	7.54
Cl	27.39, <b>34.16</b>	4.20, <b>7.13</b>	27.36, <b>28.43</b>	4.21, <b>5.78</b>	27.64, <b>30.21</b>	3.79, <b>6.48</b>	36.84	7.68
CN	27.45, <b>30.58</b>	3.78, <b>6.36</b>	27.44, <b>31.46</b>	3.71, <b>6.47</b>	27.61, <b>26.98</b>	3.44, <b>5.71</b>	37.49	7.78
COH	26.97, <b>33.54</b>	3.95, <b>7.01</b>	27.1, <b>31.17</b>	3.76, <b>4.97</b>	26.97, <b>27.82</b>	3.91, <b>5.96</b>	40.41	8.50
COCH <sub>3</sub>	26.91, <b>35.25</b>	4.16, <b>7.35</b>	27.05, <b>25.82</b>	3.89, <b>4.79</b>	26.89, <b>28.81</b>	4.09, <b>6.20</b>	33.01	6.72
CONH <sub>2</sub>	26.14, <b>33.93</b>	4.05, <b>7.06</b>	26.47, <b>31.47</b>	3.60, <b>6.53</b>	26.75, <b>30.65</b>	3.83, <b>6.64</b>	40.62	8.53
COOH	27.09, <b>38.89</b>	4.08, <b>7.12</b>	27.13, <b>28.53</b>	3.97, <b>5.91</b>	28.02, <b>29.17</b>	2.52, <b>6.28</b>	41.62	8.78
F	27.51, <b>23.87</b>	4.15, <b>4.77</b>	27.48, <b>34.04</b>	4.16, <b>7.13</b>	27.74, <b>29.78</b>	3.76, <b>6.36</b>	41.09	8.67
H	27.13, <b>37.41</b>	4.33, <b>7.82</b>	27.13, <b>37.48</b>	4.33, <b>7.83</b>	27.13, <b>30.49</b>	4.33, <b>6.62</b>	44.40	9.42
SH	26.29, <b>35.43</b>	4.95, <b>6.96</b>	26.06, <b>41.25</b>	5.23, <b>8.65</b>	26.50, <b>36.72</b>	4.25, <b>6.96</b>	45.00	9.66
OCH <sub>3</sub>	26.35, <b>35.96</b>	4.95, <b>7.44</b>	26.54, <b>35.61</b>	4.63, <b>7.45</b>	27.67, <b>33.50</b>	3.65, <b>7.21</b>	44.28	9.40
OH	26.69, <b>36.61</b>	4.69, <b>7.61</b>	26.79, <b>38.02</b>	4.64, <b>7.95</b>	27.70, <b>34.48</b>	3.77, <b>7.41</b>	45.92	9.74
NH <sub>2</sub>	26.35, <b>42.20</b>	5.51, <b>8.67</b>	26.39, <b>42.52</b>	5.62, <b>8.89</b>	27.42, <b>40.28</b>	4.13, <b>8.71</b>	38.27	8.33
NHCH <sub>3</sub>	25.87, <b>43.62</b>	5.70, <b>8.96</b>	25.88, <b>44.47</b>	5.90, <b>9.30</b>	27.00, <b>42.38</b>	4.93, <b>9.16</b>	55.83	9.40

The bold data correspond to ternary complexes T4, T5, and T6. The  $\Sigma E^2$  (in kcal mol<sup>-1</sup>) and CT (in e) values are the sum of  $E^2$  value of the  $lp_O \rightarrow \sigma_{HF}^*$  interaction and the sum of atomic charges on the X-BQ fragments, respectively.

**Table 2** The standard Gibbs free energy changes of the electron interchange reaction in the gas phase and solution media  $\Delta G^*$  (in kcal mol<sup>-1</sup>) calculated at the B3LYP/6-311++G(d,p) level of theory

X	$\Delta G^*_g$				$\Delta G^*_s$			
	X-BQ	D1	D2	D3	X-BQ	D1	D2	D3
Br	-7.33	-20.04	-19.73	-19.85	-10.53	-29.63	-29.13	-28.76
Cl	-6.66	-19.63	-19.36	-19.56	-10.04	-29.72	-29.36	-30.03
CN	-16.61	-24.54	-28.74	-28.51	-24.68	-42.83	-43.29	-42.04
COH	-13.25	-25.77	-24.90	-25.40	-20.18	-37.29	-38.14	-37.98
COCH <sub>3</sub>	-10.35	-22.42	-21.54	-22.17	-13.04	-32.99	-31.96	-32.23
CONH <sub>2</sub>	-10.72	-22.51	-21.29	-23.98	-16.87	-33.54	-31.92	-35.12
COOH	-10.21	-22.20	-21.07	-22.62	-13.72	-33.86	-32.93	-34.21
F	-5.27	-18.69	-18.73	-18.80	-8.57	-28.18	-28.26	-28.18
H	0.00	-13.87	-13.87	-13.88	0.00	-20.61	-20.60	-22.55
OCH <sub>3</sub>	4.46	-8.03	-8.22	-8.56	8.65	-11.64	-11.67	-11.45
OH	-2.16	-14.87	-14.51	-15.53	-1.14	-20.99	-20.43	-20.93
SH	-3.89	-16.40	-15.95	-16.65	-3.85	-22.57	-22.89	-23.53
NH <sub>2</sub>	14.02	2.70	2.33	2.95	28.52	12.69	14.18	14.31
NHCH <sub>3</sub>	14.78	4.17	4.04	4.10	30.44	16.30	17.95	15.67